

# Floquet controlled-phase gates in Rydberg atoms

Jun Wu,<sup>1</sup> Jin-Lei Wu,<sup>2,\*</sup> Fu-Qiang Guo,<sup>3</sup> Bing-Bing Liu,<sup>2</sup> Shi-Lei Su,<sup>2,†</sup> Xue-Ke Song,<sup>1,‡</sup> Liu Ye,<sup>1</sup> and Dong Wang<sup>1,§</sup>

<sup>1</sup>*School of Physics and Optoelectronics Engineering,  
Anhui University, Hefei 230601, People's Republic of China*

<sup>2</sup>*School of Physics, Zhengzhou University, Zhengzhou, 450001, People's Republic of China*

<sup>3</sup>*Center for Quantum Sciences and School of Physics,  
Northeast Normal University, Changchun 130024, People's Republic of China*

(Dated: January 16, 2025)

Rydberg atoms stand out as a highly promising platform for realizing quantum computation with significant advantages in constructing high-fidelity quantum gates. Floquet frequency modulation (FFM) is a potent approach for achieving resilient quantum gates through the manipulation of modulation parameters, thereby inducing intricate dynamics within quantum systems. This work introduces a method to realize controlled arbitrary phase gates in Rydberg atoms by manipulating system dynamics by the means of FFM. Notably, this method eliminates the need for laser addressing, significantly enhancing the convenience for future practical applications. Furthermore, this approach can be integrated with soft quantum control strategies to enhance the fidelity and robustness of the resultant controlled-phase gates. Finally, this methodology is applied in Grover's quantum search algorithms to prepare quantum states, demonstrating its substantial significance for future quantum information processing applications. This work leveraging Rydberg atoms and Floquet frequency modulation may herald a new era of scalable and reliable quantum computing.

## I. INTRODUCTION

Due to unique advantages, neutral atoms have emerged as one of the most promising and rapidly developing platforms in quantum computation and quantum many-body physics [1–7]. When excited to Rydberg states, neutral atoms exhibit relatively long lifetimes and strong Rydberg-Rydberg interaction (RRI) [8–11], which can manifest as the form of dipole-dipole or van der Waals forces. This interaction gives rise to the Rydberg blockade mechanism, wherein the excitation of one atom to the Rydberg state prevents the excitation of neighboring atoms [2, 12–18]. This phenomenon has been extensively utilized for the implementation of quantum logic gates [6, 19–27] and holds significant promise for various applications in quantum computing, with ongoing experimental advancements [28–30]. Furthermore, this feature allows quantum information to be encoded in the collective states of atomic ensembles, enabling the realization of mesoscopic quantum information processing and thus forming Rydberg superatoms [31–33]. Beyond the Rydberg blockade mechanism, Rydberg anti-blockade (RAB) [34–40] constitutes a critical dynamical process in neutral atomic systems, enabling the simultaneous excitation of multiple atoms to strongly interacting states. In particular, RAB permits a resonant two-photon transition between ground-state pairs and doubly excited Rydberg states in diatomic systems, thus playing a pivotal role in the realization of two-atom phase gates [41–43] and the preparation of steady-state entanglement [35, 36, 44].

In the realm of coherent quantum dynamics control, periodic driving serves as a prevalent method for state manipulation [45–50]. By applying Floquet frequency modulation (FFM), which involves periodic modulation of quantum systems at elevated frequencies, dynamic stability can be achieved [47, 51]. Furthermore, through the judicious selection of appropriate modulation amplitude and frequency, the Rabi coupling strength can be effectively regulated. This significantly enhances the dynamics of quantum systems, providing a broader array of choices for manipulating quantum systems. By periodically modulating the atom-field detuning, FFM provides a robust approach to realizing RAB dynamics, irrespective of the strength of the RRI. This technique significantly enhances RAB processes and enables the stabilization of long-lived Rydberg states with strong interactions, even for closely spaced atoms.

The practical execution of quantum computations necessitates the effective and resilient deployment of quantum logic gates [52–55] to enable the completion of numerous quantum tasks. Nevertheless, existing single dynamic protocols often fall short of meeting this demand. To address this issue, we employ the FFM method for constructing quantum logic gates. The versatile applications of FFM in coherent quantum system control allow for the exploration of diverse quantum phenomena. Through the manipulation of frequency-modulation parameters, the system dynamics can be adeptly regulated to realize robust quantum gates. Here we employ FFM to periodically modulate the atom-field detuning, thereby overcoming the constraints imposed by Rydberg anti-blockade on atomic separations. Unlike conventional approaches, which require individual laser addressing of atomic pairs to implement controlled-phase (C-Phase) gates [43], the proposed protocol facilitates the realization of a universal C-Phase gate without the atomic addressing, which significantly enhances the experimental

\* jlwu517@zzu.edu.cn

† slsu@zzu.edu.cn

‡ songxk@ahu.edu.cn

§ dwang@ahu.edu.cn

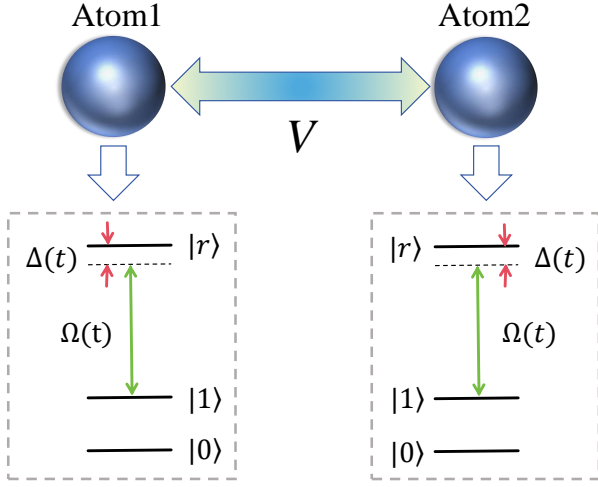


FIG. 1. The schematic illustration depicts the energy level configuration of two Rydberg atoms. Each atom comprises two hyperfine ground states, denoted as  $|0\rangle$  and  $|1\rangle$ , alongside a Rydberg excited state represented by  $|r\rangle$ . Simultaneously, both atoms undergo excitation from state  $|1\rangle$  to state  $|r\rangle$  with Rabi frequency  $\Omega(t)$  and detuning  $\Delta(t)$ , while exhibiting Rydberg interactions between their respective  $|r\rangle$  states.

feasibility and operational efficiency. Simultaneously, owing to the intricate dynamics inherent in the Floquet system, varied modulation parameters can be selected to individually achieve the universal C-Phase gate. This offers a broader array of options for the construction of quantum logic gates. Furthermore, the constructed C-Phase gate can be integrated with Gaussian soft quantum control optimization techniques [56–63], thereby improving the fidelity of the C-Phase gate and mitigating the occurrence of undesirable high-frequency oscillations during the evolution process. In addition, in the realm of quantum computing, Grover’s search algorithms have exhibited notable advantages [64–73]. By modulating phase rotation instead of phase inversion, the high success-rate target search can be effectively realized [66]. Our approach facilitates multi-item searching with a unit success probability, eliminating the necessity for individual addressing and simplification of the quantum circuit offers a promising and feasible avenue for the practical implementation of the algorithm.

## II. MODEL AND HAMILTONIAN

As illustrated in Fig. 1, we initially examine a scenario involving two neutral atoms interacting via Rydberg interactions. Each atom is stimulated from the hyperfine ground state  $|1\rangle$  to the Rydberg excited state  $|r\rangle$  with Rabi frequency denoted as  $\Omega(t)e^{i\phi(t)}$  and detuning  $\Delta(t)$ . In the interaction picture with rotating-wave approximation (RWA), the evolution of the system is governed by the Hamiltonian ( $\hbar \equiv 1$ ).

$$\hat{H}(t) = -\Delta(t) \sum_{i=1}^2 |r\rangle_i \langle r| + \frac{\Omega(t)}{2} e^{i\phi(t)} \sum_{i=1}^2 (|1\rangle_i \langle r| + \text{H.c.}) + V |rr\rangle \langle rr|, \quad (1)$$

where  $i$  indexes the  $i$ -th atom,  $V$  represents the RRI strength, and the laser detuning  $\Delta(t) = \Delta_0 + \delta \sin(\omega_0 t)$  undergoes sinusoidal FFM with the modulation frequency  $\omega_0$  and the modulation amplitude  $\delta$ . The notation  $|ab\rangle \equiv |a\rangle_1 \otimes |b\rangle_2$  is employed throughout this study for conciseness. In implementing FFM, we can utilize a Rydberg excitation laser controlled by an acoustic-optic modulator (AOM) driven by an arbitrary waveform generator (AWG). Unlike conventional Floquet engineering techniques, FFM does not rely on periodic pulses, instead, it directly alters the effective coupling between energy levels [74, 75].

Now we introduce the unitary operator,  $\hat{U}(t) = \exp[-if(t) \sum_{i=1}^2 |r\rangle_i \langle r| - iVt |rr\rangle \langle rr|]$  with  $f(t) = -\Delta_0 t + \delta/\omega_0 \cos(\omega_0 t)$ , the Hamiltonian (1) is transformed into  $\hat{H}'(t) = i\hbar \hat{U}^\dagger(t) \hat{U}(t) + \hat{U}^\dagger(t) \hat{H} \hat{U}(t)$ , calculated as

$$\hat{H}'(t) = \frac{\Omega(t)}{2} e^{i[\phi(t)+f(t)]} \left[ (\sqrt{2}|W\rangle \langle 11| + |0r\rangle \langle 01| + |r0\rangle \langle 10|) + \sqrt{2} e^{iVt} |rr\rangle \langle W| \right] + \text{H.c.}, \quad (2)$$

in which the intermediate state is denoted as  $|W\rangle = (|1r\rangle + |r1\rangle)/\sqrt{2}$ . We introduce the modulation index  $\alpha = \delta/\omega_0$  and assume  $\Delta_0 = 0$  for simplicity. By employing the Jacobi-Anger expansion  $\exp[\pm i\alpha \cos \omega_0 t] = \sum_{m=-\infty}^{\infty} J_m(\alpha) \exp[\pm im(\omega_0 t + \pi/2)]$ , the modified Hamiltonian  $\hat{H}'(t)$  can be expressed as

$$\hat{H}'(t) = \frac{\Omega(t)}{2} e^{i\phi(t)} \sum_{m=-\infty}^{\infty} J_m(\alpha) e^{im\omega_0 t + im\frac{\pi}{2}} \left[ (|0r\rangle \langle 01| + |r0\rangle \langle 10| + \sqrt{2}|W\rangle \langle 11|) + \sqrt{2} e^{iVt} |rr\rangle \langle W| \right] + \text{H.c.}, \quad (3)$$

where  $J_m(\alpha)$  represents the  $m$ th order Bessel function of the first kind. To simplify subsequent analyses, the Rabi frequencies between the states are individually rescaled to

$$\Omega_a(t) = \Omega(t) e^{i\phi(t)} \sum_{m=-\infty}^{\infty} J_m(\alpha) e^{im\omega_0 t + im\frac{\pi}{2}},$$

$$\Omega_b(t) = \Omega(t) e^{i\phi(t)} \sum_{m=-\infty}^{\infty} J_m(\alpha) e^{i(m\omega_0 + V)t + im\frac{\pi}{2}}. \quad (4)$$

By selecting a significantly high modulation frequency  $\omega_0$ , the Rabi frequencies  $\Omega_a(t)$  and  $\Omega_b(t)$  are predominantly influenced by the resonance term. Specifically, the Rabi frequency  $\Omega_a(t)$  is governed by  $J_0(\alpha)$ , whereas for  $\Omega_b(t)$ , we establish  $m\omega_0 = -V$  to satisfy the resonance criterion.

For a more intuitive analysis, we partition the system dynamics into distinct sectors, specifically involving the

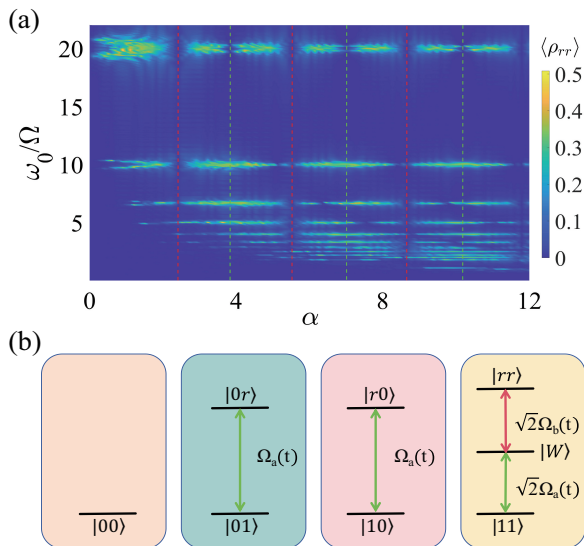


FIG. 2. (a) Schematic illustrating the impact of FFM on Rydberg anti-blockade dynamics. The time-average population of  $|rr\rangle$  varies as a function of the modulation index  $\alpha$  and the normalized modulation frequency  $\omega_0/\Omega$ . The red and green dashed curves correspond to  $J_0(\alpha) = 0$  and  $J_1(\alpha) = 0$ , respectively. (b) Dynamics of transitions among the four ground states: the  $|00\rangle$  state remains unaltered, transitions of the  $|01\rangle$  and  $|10\rangle$  states exhibit Rabi oscillations with the same Rabi frequency  $\Omega_a(t)$ , while the  $|11\rangle$  state is excited to the  $|rr\rangle$  state via the intermediate state  $|W\rangle$  with equivalent Rabi frequencies of  $\sqrt{2}\Omega_a(t)$  and  $\sqrt{2}\Omega_b(t)$ , respectively.

computational states  $|00\rangle$ ,  $|01\rangle$ ,  $|10\rangle$ , and  $|11\rangle$ . The state  $|00\rangle$  remains unchanged as  $|0\rangle$  is decoupled to the driving field. In the cases of the initial states  $|01\rangle$  and  $|10\rangle$ , the dynamics of system can be described by the two-level system with the Hamiltonian, respectively

$$\begin{aligned}\hat{H}_{01}(t) &= \frac{\Omega_a(t)}{2}|01\rangle\langle 0r| + \text{H.c.}, \\ \hat{H}_{10}(t) &= \frac{\Omega_a(t)}{2}|10\rangle\langle r0| + \text{H.c.}\end{aligned}\quad (5)$$

For the initial state  $|11\rangle$ , the system dynamics can be described by the equivalent three-level system with the Hamiltonian

$$\hat{H}_{11}(t) = \frac{\sqrt{2}\Omega_a(t)}{2}|11\rangle\langle W| + \frac{\sqrt{2}\Omega_b(t)}{2}|W\rangle\langle rr| + \text{H.c.} \quad (6)$$

### III. C-PHASE GATE OF TWO RYDBERG ATOMS

In this section, we utilize the FFM scheme to construct a universal two-qubit C-Phase gate, capitalizing on its intricate dynamics. By varying the modulation index  $\alpha$  and modulation frequency  $\omega_0$ , we present the average population of the doubly excited Rydberg state  $|rr\rangle$  within  $10 \mu\text{s}$  in Fig. 2(a) with the RRI strength of  $V = 20 \Omega$ . The results indicate that the FFM scheme

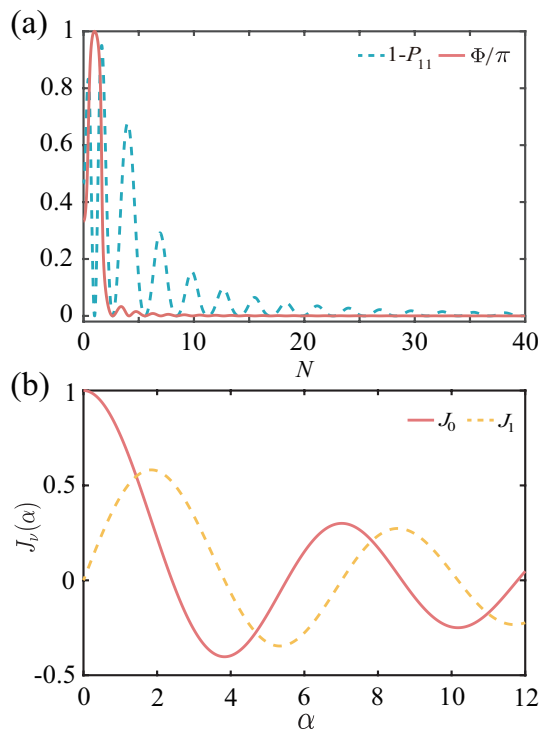


FIG. 3. (a) Diagram illustrating the variations in population and phase of  $|11\rangle$  as the ratio  $N$  of  $|\Omega_b(t)|$  to  $|\Omega_a(t)|$  is altered. (b) Evolution of the Bessel function of the first kind with respect to the modulation index  $\alpha$ , denoting  $J_0$  and  $J_1$  as the zeroth and first order Bessel functions of the first kind, respectively.

can effectively manipulate the dynamic behavior of system according to the population behaviors of  $|rr\rangle$ . Notably, when the resonance condition  $\omega_0 = V$  is satisfied, the population of the  $|rr\rangle$  state is primarily modulated by  $J_0(\alpha)$  and  $J_1(\alpha)$ . By selecting values of  $\alpha$  at which either  $J_0(\alpha)$  or  $J_1(\alpha)$  vanishes, the population of  $|rr\rangle$  state can be effectively suppressed.

To construct the desired two-qubit controlled-phase gate  $\hat{U}_{CP} = \text{diag}(1, -e^{i\vartheta}, -e^{i\vartheta}, 1)$ , we employ two identical Rydberg global pulses with equal duration  $\tau = \pi/|\Omega_a(t)|$ , with a laser phase jump  $\vartheta$  inserted between the two pulses. Utilizing the unitary operator  $\hat{U}_f = \exp(-i \int_0^\tau \hat{H}_i(t) dt)$ , where  $i = 01, 10, 11$ , each pulse induces a transformation in the atomic states. An in-depth exploration into the evolution of the four computational basis states under the impact of  $\hat{U}_{CP}$  is presented in Fig. 2(b). The state  $|00\rangle$  is unaffected by these pulses with  $\hat{U}_f|00\rangle = |00\rangle$ , the states  $|01\rangle$  and  $|10\rangle$  return to themselves with an additional phase factor represented by  $\hat{U}_f|01\rangle(|10\rangle) = -e^{i\vartheta}|01\rangle(|10\rangle)$  after a duration of  $2\tau$ . Lastly, concerning the evolution of the state  $|11\rangle$ , our objective is to return to the same state without accumulating any phase after the complete evolution. This is achieved by appropriately selecting the time-dependent functions  $|\Omega_a(t)|$  and  $|\Omega_b(t)|$ . Thus, we define  $|\Omega_b(t)|$  as  $N$  times  $|\Omega_a(t)|$  and evaluate the time evolution operator  $\hat{U}_{11}$  for the corresponding three-

level system using Eq. (6). By applying the condition  $\hat{U}_{11}|11\rangle = |11\rangle$ , we can analyze the changes in population  $P_{11}$  and phase  $\Phi_{11}$  of the state  $|11\rangle$  as  $N$  varies. The curves depicting the variations of  $P_{11}$  and  $\Phi_{11}$  for  $N \in [0, 20]$  are illustrated in Fig. 3(a). The plot reveals that for  $N = (\sqrt{31} - \sqrt{7})n + \sqrt{7}$ ,  $n = 0, 1, 2, \dots$ , the state  $|11\rangle$  undergoes self-evolution without accumulating any additional phase. With increasing  $n$ , the population of the  $|11\rangle$  state remains close to 1 due to the significant disparity between  $|\Omega_b(t)|$  and  $|\Omega_a(t)|$ . This intriguing behavior, similar to the unconventional Rydberg pumping mechanism [76], effectively freezes the evolution of a two-atom system featuring the same ground states.

To satisfy the resonance conditions detailed in Eq. (4), we assign  $\omega_0 = V$  such that the coupling strength between the  $|W\rangle$  state and  $|rr\rangle$  state is primarily influenced by  $J_1(\alpha)$ , while the Rabi frequency between the  $|11\rangle$  state and  $|W\rangle$  state is predominantly governed by  $J_0(\alpha)$ . This configuration ensures that  $|\Omega_b(t)| = N|\Omega_a(t)|$  is equivalent to  $J_1(\alpha) = NJ_0(\alpha)$ , enabling us to select a suitable modulation index  $\alpha$  to attain the desired nontrivial two-qubit gate illustrated in Fig. 3(b). The aforementioned FFM approach facilitates the realization of the two-qubit C-Phase gate:  $\hat{U}_{CP} = \text{diag}(1, -e^{i\vartheta}, -e^{i\vartheta}, 1)$  in reference to the computational basis  $\{|00\rangle, |01\rangle, |10\rangle, |11\rangle\}$ .

#### IV. GATE FIDELITY, OPTIMAL CONTROL AND ROBUSTNESS

##### A. PARAMETER SELECTION AND NUMERICAL METHODS

In this section, we employ feasible experimental parameters to conduct a numerical simulation of the performance of our FFM scheme. For  $T_a = 10 \mu\text{K}$ , the lifetime  $\tau_r$  of the Rydberg state  $|r\rangle$  in  $^{87}\text{Rb}$  atoms with a principal quantum number 70 is approximately  $400 \mu\text{s}$ . The effective Rabi frequency of the two-photon process is  $\Omega = 2\pi \times 3.5 \text{ MHz}$ , and the strength of the Rydberg-Rydberg interaction is denoted as  $V = 2\pi \times 70.18 \text{ MHz}$ , considering an interatomic separation of  $d = 4.8 \mu\text{m}$  [6, 77, 78].

To study evolution of the two-atom system in the presence of noise, we utilize the Lindblad master equation to assess the gate efficacy under dissipative effects, expressed as

$$\frac{\partial \hat{\rho}(t)}{\partial t} = -\frac{i}{\hbar} [\hat{H}(t), \hat{\rho}(t)] + \mathcal{L}_r[\hat{\rho}] \quad (7)$$

where  $\hat{\rho}(t)$  represents the density matrix operator corresponding to the two-atom system,  $\hat{H}(t)$  stands for the time-varying Hamiltonian of the system as depicted in Eq. (1), and the dissipation terms  $\mathcal{L}_r[\hat{\rho}]$  account for the spontaneous decay originating from the strongly-interacting states, elucidated as

$$\mathcal{L}_r[\hat{\rho}] = \sum_{i=1,2} \sum_{j=0,1} (\hat{L}_j^i \hat{\rho} \hat{L}_j^{i\dagger} - \frac{1}{2} \hat{L}_j^{i\dagger} \hat{L}_j^i \hat{\rho} - \frac{1}{2} \hat{\rho} \hat{L}_j^i \hat{L}_j^{i\dagger}) \quad (8)$$

in which the Lindblad operators  $\hat{L}_j^i = \sqrt{\gamma_j} |j\rangle_i \langle r|$  represent the jump operators characterizing the spontaneous emission of the atom from the Rydberg state  $|r\rangle$  to a ground state  $|j\rangle$ , where  $\gamma_j$  represents the decay rate.

To demonstrate the efficacy and resilience of our proposed two-qubit C-Phase gate across diverse initial conditions, we evaluate the average fidelity [79]

$$\bar{F}(\xi, \hat{U}) = \frac{\sum_k \text{tr}[\hat{U} \hat{U}_k^\dagger \hat{U}^\dagger \xi(\hat{U}_k)] + d_k^2}{d_k^2(d_k + 1)}, \quad (9)$$

in which  $\hat{U}$  represents the perfect logic gate,  $\hat{U}_k$  stands for the tensor of Pauli matrices  $\hat{I}\hat{I}, \hat{I}\hat{\sigma}_x, \hat{I}\hat{\sigma}_y, \hat{I}\hat{\sigma}_z, \dots, \hat{\sigma}_z\hat{\sigma}_z$  for a two-qubit gate,  $d_k = 2^x$ , with  $x$  being the number of qubits in a quantum gate and in this case,  $d_k = 4$ .  $\xi(\hat{U}_k)$  denotes the trace-preserving quantum operation achieved by solving the master equation (7).

In Fig. 4(a), we present the average fidelity of the C-Phase gate with  $\vartheta = \pi/2$  for  $n = 0, 1, 2$  corresponding to the gate time  $T = 2\pi/|\Omega_a(t)|$ , yielding average fidelities of 0.9973, 0.9870, and 0.9856, respectively. It can be observed that for  $n = 0$ , the achieved gate fidelity is the highest with the shortest gate time. Conversely, for  $n = 1$  and 2, the gate time increases due to the decreasing values of selected  $J_0(\alpha)$  and  $J_1(\alpha)$ , leading to a

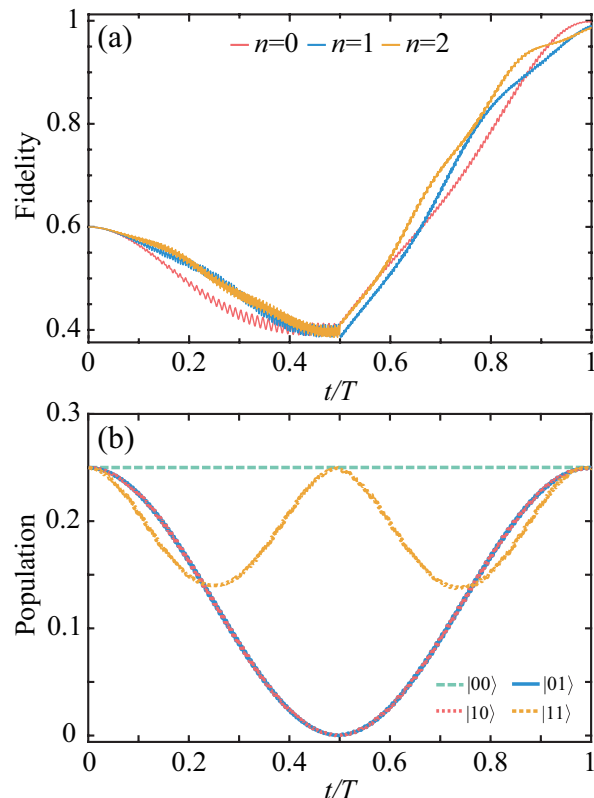


FIG. 4. (a) The evolution of the average gate fidelity of the implemented C-Phase gate over time, when  $n$  equals 0,1,2. (b) Dynamics of the population distribution among the four computational states for the scenario where  $n = 0$ . The time-independent Rabi frequency  $\Omega = 2\pi \times 3.5 \text{ MHz}$ ,  $V = \omega_0 = 2\pi \times 70.18 \text{ MHz}$ , and the gate duration being  $T = 2\pi/|\Omega_a(t)|$ .



decline in the gate fidelity influenced by the disregarded non-resonant terms. Furthermore, for  $n = 0$ , we simulate the population evolution of the four computational states displayed in Fig. 4(b) by initializing a superposition  $|\psi\rangle = (|00\rangle + |01\rangle + |10\rangle + |11\rangle)/2$ , it can be observed that the evolution of the four computational basis subspaces is in agreement with the analysis.

## B. GAUSSIAN SOFT CONTROL

Observing from Fig. 4(a), we note that the fidelity evolution exhibits pronounced oscillations due to imperfect parameter settings aimed at mitigating the high-frequency oscillations, following the defective RWA. These substantial oscillations render the resultant C-Phase gate particularly susceptible to errors in the Rabi frequency. To address this issue, we leverage soft quantum control techniques [56] to refine the parameters for better adherence to RWA conditions, thus damping the high-frequency oscillatory effects and reducing parameter uncertainties during the preparation phase, ultimately enhancing the gate fidelity.

Under the implementation of soft quantum control, the time-independent square pulse (SP) with Rabi frequency  $\Omega$  can be transformed into a time-evolving Gaussian pulse (GP), given by  $\Omega_g(t) = \Omega \exp[-(t - 3T_g)^2/T_g^2]$ , where  $\Omega$  and  $T_g$  denote the maximum amplitude and width of GP, respectively. Ensuring the pulse area remains constant, we deduce  $T_g = 2\sqrt{\pi}/|\Omega_a(t)|$  by satisfying  $\int_0^{t_g} \Omega_g(t) dt = 2\pi$  with  $t_g = 6T_g$ . Employing this GP configuration, we illustrate the average gate fidelity and population dynamics of the C-Phase gate for the case  $n = 0$  in Figs. 5(a) and 5(b). The results depict a substantial reduction in oscillations through Gaussian soft quantum control, elevating the average fidelity to 0.9982. Moreover, GP offer practical advantages over traditional SP in experimental scenarios. Consequently, the fusion of our approach with Gaussian soft control significantly enhances operational feasibility in experiments, showcasing promising and valuable applications.

## C. RESILIENCE TO EXPERIMENTAL IMPERFECTIONS

The excitation process from the ground state  $|1\rangle$  to the Rydberg state  $|r\rangle$  can be achieved via a two-photon mechanism in Rb atoms [6, 78]. Within the FFM scheme, to meet the condition  $V = \omega_0 \gg \Omega$ , it is necessary to have Rydberg states characterized by sufficiently high principal quantum numbers or close interatomic separations to ensure a potent Rydberg-Rydberg interaction (RRI) strength. Hence, we consider  $^{87}\text{Rb}$  atoms interacting through van der Waals forces. The energy levels are set as two hyperfine ground states  $|0\rangle = |5S_{1/2}, F = 1, m_F = 1\rangle$  and  $|1\rangle = |5S_{1/2}, F = 2, m_F = 2\rangle$  [80], an intermediary state  $|p\rangle = |5p_{3/2}\rangle$  or  $|p\rangle = |6p_{3/2}\rangle$ , and the Rydberg strongly-interacting state  $|r\rangle = |70S_{1/2}\rangle$  possessing an

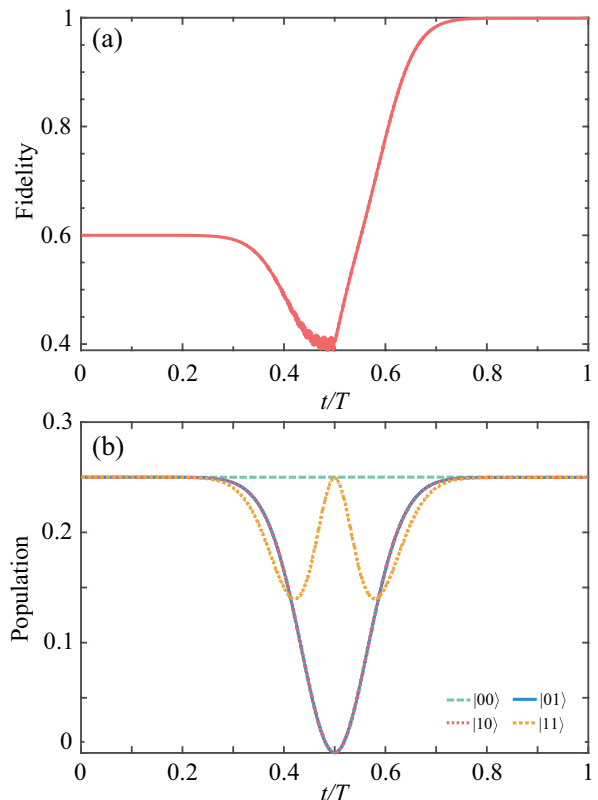


FIG. 5. (a) The temporal progression of the average gate fidelity for the C-Phase gate utilizing Gaussian soft quantum control when  $n = 0$ . (b) Evolution of the population distribution among the four computational states corresponding to the C-Phase gate. The time-dependent Rabi frequency is given by  $\Omega_g(t) = \Omega \exp[-(t - 3T_g)^2/T_g^2]$  with  $\Omega = 2\pi \times 3.5$  MHz,  $T_g = 2\sqrt{\pi}/|\Omega_a(t)|$  and a gate time of  $t_g = 6T_g$ . Additionally,  $V = \omega_0 = 2\pi \times 70.18$  MHz.

interaction coefficient of  $C_6/2\pi = 858.4$  GHz  $\mu\text{m}^6$ . Considering an interatomic separation of  $d = 4.8$   $\mu\text{m}$ , this setup results in a RRI strength of  $V = 2\pi \times 70.18$  MHz for the specified Rydberg states.

Subsequently, we delve into the robustness of the constructed C-Phase gates against parameter inaccuracies, with a particular focus on the impact of laser intensity on the fidelity of the C-Phase gate. To explore this scenario, we examine the effects of deviations in the Rabi frequency  $\Omega$ , encompassing both upward and downward deviations. To quantify these deviations, we introduce the deviation value  $\delta\Omega$  and the relative error  $\delta\Omega/\Omega$ . Subsequently, we analyze the influence of relative errors on the average gate fidelity when employing either SP or GP for the laser configuration, as illustrated in Fig. 6. Notably, when the parameters fluctuate within a 10% range, the average fidelity of the C-Phase gates for both schemes exhibits gradual decrease, affirming the robustness of our proposed protocol.

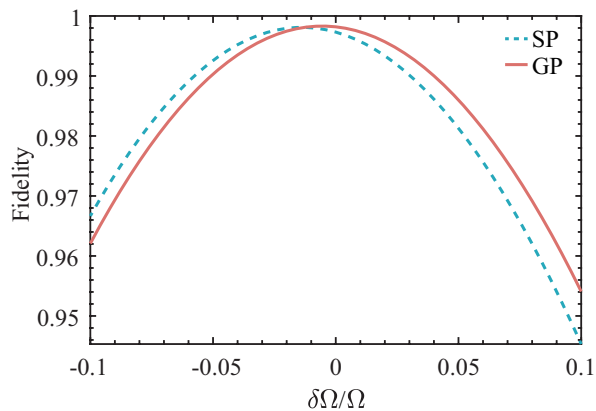


FIG. 6. The impact of relative errors in the Rabi frequency on gate fidelity is examined using square pulse and Gaussian pulse configurations. The relevant parameters remain consistent with  $V = \omega_0 = 2\pi \times 70.18$  MHz,  $\Omega = 2\pi \times 3.5$  MHz, and the time-dependent Rabi frequency  $\Omega_g(t) = \Omega \exp[-(t - 3T_g)^2/T_g^2]$  as previously described.

## V. APPLICATION IN LONG'S ALGORITHM

Finally, we consider to apply the proposed C-Phase gates in implementing the multi-item quantum search algorithm. According to Long's algorithm [68, 81], by replacing the phase inversion with phase rotation in oracle and diffusion-operation, the desired target items can be searched with zero failure rate. The detailed circuit diagram is presented in Fig. 7(a), together with the following steps.

(i) Starting with the initial state  $\frac{1}{2}(|00\rangle + |01\rangle + |10\rangle + |11\rangle)$ , the oracle operator is applied to mark the target items. For the one-item search targeting the state  $|11\rangle$ , the oracle operator is defined as  $U_1 = |00\rangle\langle 00| + |01\rangle\langle 01| + |10\rangle\langle 10| - |11\rangle\langle 11|$ , which is implemented by selecting  $\vartheta = \pi/2$  in C-Phase gate together with the single-qubit operator  $U = |0\rangle\langle 0| + i|1\rangle\langle 1|$  applied to both qubits. For the two-item target state  $(|01\rangle + |10\rangle)/\sqrt{2}$ , the oracle operator is given by  $U_1 = |00\rangle\langle 00| + i|01\rangle\langle 01| + i|10\rangle\langle 10| + |11\rangle\langle 11|$ , which is realized by setting  $\vartheta = -\pi/2$  in C-Phase gate.

(ii) For the diffusion operator, the inverse Hadamard operation ( $H^\dagger$ ) is initially applied to each qubit. The operator  $U_2$  is identical to  $U_1$  in the case of the one-item search. However, for the two-item search,  $U_2$  is defined as  $|00\rangle\langle 00| + |01\rangle\langle 01| + |10\rangle\langle 10| + i|11\rangle\langle 11|$ , which is implemented by setting  $\vartheta = -5\pi/4$  in C-Phase gate together with the single qubit operation  $U = |0\rangle\langle 0| + e^{i\pi/4}|1\rangle\langle 1|$  applied to each qubit. Finally, the Hadamard operation is applied to each qubit to complete the diffusion process.

Following these steps, the one-item and two-item searches are successfully implemented, with the dynamical processes are illustrated in Figs. 7(b) and 7(c). The

achieved fidelities of 0.9983 for the one-item search and 0.9953 for the two-item search underscore the effectiveness of our scheme. Notably, the proposed approach simplifies the circuit design and eliminates the need for individual addressing in two-qubit operations, thereby significantly improving the accuracy and efficiency of the quantum search algorithms.

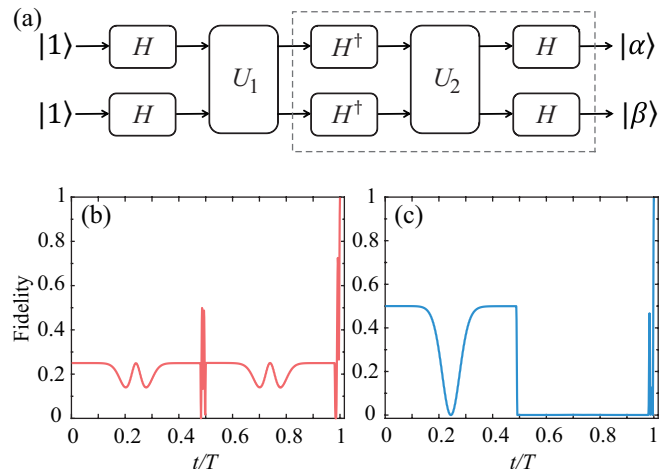


FIG. 7. (a) The quantum circuit depicting the search algorithm for both one-item and two-item scenarios. (b) The fidelity evolution of the target state in the search algorithm for a one-item over time. (c) Temporal variation diagram illustrating the fidelity of the target state in a search algorithm for two-item.

## VI. CONCLUSION

We have introduced a strategy to realize a C-Phase gate utilizing Rydberg atoms and employing FFM techniques. This approach is implemented through the Floquet periodic modulation of the atom-field detuning. By employing this method, the constraints posed by the distance between Rydberg atoms on the interaction strength can be surpassed, while also allowing for the convenient adjustment of pertinent parameters to tailor the dynamics of quantum systems. This capability is particularly advantageous for the development of quantum logic gates. With respect to the most recent experimental parameters concerning the alkali metal rubidium atom, the C-Phase gates devised by our proposed approach exhibit outstanding performances. Furthermore, our method can be integrated with Gaussian soft quantum control techniques to enhance the fidelity and robustness of the C-Phase gate. Ultimately, our C-Phase holds promise for search algorithms with high success rates, thereby significantly enhancing the efficacy of multi-qubit operations without the necessity for laser independent addressing.

[1] D. Jaksch, J. I. Cirac, P. Zoller, S. L. Rolston, R. Côté, and M. D. Lukin, "Fast quantum gates for neutral

atoms," *Phys. Rev. Lett.* **85**, 2208–2211 (2000).

- [2] Thomas F. Gallagher, *Rydberg Atoms*, Cambridge Monographs on Atomic, Molecular and Chemical Physics (Cambridge University Press, 1994).
- [3] M. Saffman, T. G. Walker, and K. Mølmer, “Quantum information with rydberg atoms,” *Rev. Mod. Phys.* **82**, 2313–2363 (2010).
- [4] L. Béguin, A. Vernier, R. Chicireanu, T. Lahaye, and A. Browaeys, “Direct measurement of the van der waals interaction between two rydberg atoms,” *Phys. Rev. Lett.* **110**, 263201 (2013).
- [5] A. Omran, H. Levine, A. Keesling, G. Semeghini, T. T. Wang, S. Ebadi, H. Bernien, A. S. Zibrov, H. Pichler, S. Choi, J. Cui, M. Rossignolo, P. Rembold, S. Montanero, T. Calarco, M. Endres, M. Greiner, V. Vuletić, and M. D. Lukin, “Generation and manipulation of schrödinger cat states in rydberg atom arrays,” *Science* **365**, 570–574 (2019).
- [6] Harry Levine, Alexander Keesling, Giulia Semeghini, Ahmed Omran, Tout T. Wang, Sepehr Ebadi, Hannes Bernien, Markus Greiner, Vladan Vuletić, Hannes Pichler, and Mikhail D. Lukin, “Parallel implementation of high-fidelity multiqubit gates with neutral atoms,” *Phys. Rev. Lett.* **123**, 170503 (2019).
- [7] Simon J. Evered, Dolev Bluvstein, Marcin Kalinowski, Sepehr Ebadi, Tom Manovitz, Hengyun Zhou, Sophie H. Li, Alexandra A. Geim, Tout T. Wang, Nishad Maskara, Harry Levine, Giulia Semeghini, Markus Greiner, Vladan Vuletić, and Mikhail D. Lukin, “High-fidelity parallel entangling gates on a neutral-atom quantum computer,” *Nature* **622**, 268–272 (2023).
- [8] Shraddha Anand, Conor E. Bradley, Ryan White, Vikram Ramesh, Kevin Singh, and Hannes Bernien, “A dual-species rydberg array,” *Nature Physics* **20**, 1744–1750 (2024).
- [9] Valerio Crescimanna, Jacob Taylor, Aaron Z. Goldberg, and Khabat Heshami, “Quantum control of rydberg atoms for mesoscopic quantum state and circuit preparation,” *Phys. Rev. Appl.* **20**, 034019 (2023).
- [10] Zhu-yao Jin and Jun Jing, “Geometric quantum gates via dark paths in rydberg atoms,” *Phys. Rev. A* **109**, 012619 (2024).
- [11] Chi-En Wu, Teodora Kirova, Marcis Auzins, and Yi-Hsin Chen, “Rydberg-rydberg interaction strengths and dipole blockade radii in the presence of f&#x00f6;rster resonances,” *Opt. Express* **31**, 37094–37104 (2023).
- [12] M. D. Lukin, M. Fleischhauer, R. Cote, L. M. Duan, D. Jaksch, J. I. Cirac, and P. Zoller, “Dipole blockade and quantum information processing in mesoscopic atomic ensembles,” *Phys. Rev. Lett.* **87**, 037901 (2001).
- [13] E. Urban, T. A. Johnson, T. Henage, L. Isenhower, D. D. Yavuz, T. G. Walker, and M. Saffman, “Observation of rydberg blockade between two atoms,” *Nature Physics* **5**, 110–114 (2009).
- [14] T. M. Graham, M. Kwon, B. Grinkemeyer, Z. Marra, X. Jiang, M. T. Lichtman, Y. Sun, M. Ebert, and M. Saffman, “Rydberg-mediated entanglement in a two-dimensional neutral atom qubit array,” *Phys. Rev. Lett.* **123**, 230501 (2019).
- [15] Charles Fromenteil, Dolev Bluvstein, and Hannes Pichler, “Protocols for rydberg entangling gates featuring robustness against quasistatic errors,” *PRX Quantum* **4**, 020335 (2023).
- [16] Vikas Buchemavari, Sivaprasad Omanakuttan, Yuan-Yu Jau, and Ivan Deutsch, “Entangling quantum logic gates in neutral atoms via the microwave-driven spin-flip blockade,” *Phys. Rev. A* **109**, 012615 (2024).
- [17] Yuan Sun, “Buffer-atom-mediated quantum logic gates with off-resonant modulated driving,” *Science China Physics, Mechanics & Astronomy* **67**, 120311 (2024).
- [18] Zi-Yuan Chen, Jia-Hao Liang, Zhao-Xin Fu, Hong-Zhi Liu, Ze-Rui He, Meng Wang, Zhi-Wei Han, Jia-Yi Huang, Qing-Xian Lv, and Yan-Xiong Du, “Single-pulse two-qubit gates for rydberg atoms with noncyclic geometric control,” *Phys. Rev. A* **109**, 042621 (2024).
- [19] L. Isenhower, E. Urban, X. L. Zhang, A. T. Gill, T. Henage, T. A. Johnson, T. G. Walker, and M. Saffman, “Demonstration of a neutral atom controlled-not quantum gate,” *Phys. Rev. Lett.* **104**, 010503 (2010).
- [20] S.-L. Su, Li-Na Sun, B.-J. Liu, L.-L. Yan, M.-H. Yung, W. Li, and M. Feng, “Rabi- and blockade-error-resilient all-geometric rydberg quantum gates,” *Phys. Rev. Appl.* **19**, 044007 (2023).
- [21] Ditte Møller, Lars Bojer Madsen, and Klaus Mølmer, “Quantum gates and multiparticle entanglement by rydberg excitation blockade and adiabatic passage,” *Phys. Rev. Lett.* **100**, 170504 (2008).
- [22] Bao-Jie Liu, Shi-Lei Su, and Man-Hong Yung, “Nonadiabatic noncyclic geometric quantum computation in rydberg atoms,” *Phys. Rev. Res.* **2**, 043130 (2020).
- [23] Ming Xue, Shijie Xu, Xinwei Li, and Xiangliang Li, “High-fidelity and robust controlled- $z$  gates implemented with rydberg atoms via echoing rapid adiabatic passage,” *Phys. Rev. A* **110**, 032619 (2024).
- [24] F.-Q. Guo, J.-L. Wu, X.-Y. Zhu, Z. Jin, Y. Zeng, S. Zhang, L.-L. Yan, M. Feng, and S.-L. Su, “Complete and nondestructive distinguishing of many-body rydberg entanglement via robust geometric quantum operations,” *Phys. Rev. A* **102**, 062410 (2020).
- [25] Anupam Mitra, Sivaprasad Omanakuttan, Michael J. Martin, Grant W. Biedermann, and Ivan H. Deutsch, “Neutral-atom entanglement using adiabatic rydberg dressing,” *Phys. Rev. A* **107**, 062609 (2023).
- [26] Sven Jandura, Jeff D. Thompson, and Guido Pupillo, “Optimizing rydberg gates for logical-qubit performance,” *PRX Quantum* **4**, 020336 (2023).
- [27] P.-Y. Song, J.-F. Wei, Peng Xu, L.-L. Yan, M. Feng, Shi-Lei Su, and Gang Chen, “Fast realization of high-fidelity nonadiabatic holonomic quantum gates with a time-optimal-control technique in rydberg atoms,” *Phys. Rev. A* **109**, 022613 (2024).
- [28] Alec Cao, William J. Eckner, Theodor Lukin Yelin, Aaron W. Young, Sven Jandura, Lingfeng Yan, Kyungtae Kim, Guido Pupillo, Jun Ye, Nelson Darkwah Oppong, and Adam M. Kaufman, “Multi-qubit gates and schrödinger cat states in an optical clock,” *Nature* **634**, 315–320 (2024).
- [29] Zhubing Jia, William Huie, Lintao Li, Won Kyu Calvin Sun, Xiye Hu, Aakash, Healey Kogan, Abhishek Karve, Jong Yeon Lee, and Jacob P. Covey, “An architecture for two-qubit encoding in neutral ytterbium-171 atoms,” *npj Quantum Information* **10**, 106 (2024).
- [30] G. Unnikrishnan, P. Ilzhöfer, A. Scholz, C. Hölzl, A. Götzelmann, R. K. Gupta, J. Zhao, J. Krauter, S. Weber, N. Makki, H. P. Büchler, T. Pfau, and F. Meinert, “Coherent control of the fine-structure qubit in a single alkaline-earth atom,” *Phys. Rev. Lett.* **132**, 150606 (2024).
- [31] Nina Stiesdal, Jan Kumlin, Kevin Kleinbeck, Philipp Lunt, Christoph Braun, Asaf Paris-Mandoki, Christoph

- Tresp, Hans Peter Büchler, and Sebastian Hofferberth, “Observation of three-body correlations for photons coupled to a rydberg superatom,” *Phys. Rev. Lett.* **121**, 103601 (2018).
- [32] Johannes Zeiher, Peter Schauß, Sebastian Hild, Tommaso Macrì, Immanuel Bloch, and Christian Gross, “Microscopic characterization of scalable coherent rydberg superatoms,” *Phys. Rev. X* **5**, 031015 (2015).
- [33] Xiao-Qiang Shao, Shi-Lei Su, Lin Li, Rejish Nath, Jin-Hui Wu, and Weibin Li, “Rydberg superatoms: An artificial quantum system for quantum information processing and quantum optics,” *Applied Physics Reviews* **11**, 031320 (2024).
- [34] C. Ates, T. Pohl, T. Pattard, and J. M. Rost, “Antiblockade in rydberg excitation of an ultracold lattice gas,” *Phys. Rev. Lett.* **98**, 023002 (2007).
- [35] D. D. Bhaktavatsala Rao and Klaus Mølmer, “Dark entangled steady states of interacting rydberg atoms,” *Phys. Rev. Lett.* **111**, 033606 (2013).
- [36] A. W. Carr and M. Saffman, “Preparation of entangled and antiferromagnetic states by dissipative rydberg pumping,” *Phys. Rev. Lett.* **111**, 033607 (2013).
- [37] Thomas Amthor, Christian Giese, Christoph S. Hofmann, and Matthias Weidemüller, “Evidence of antiblockade in an ultracold rydberg gas,” *Phys. Rev. Lett.* **104**, 013001 (2010).
- [38] Fangli Liu, Zhi-Cheng Yang, Przemyslaw Bienias, Thomas Iadecola, and Alexey V. Gorshkov, “Localization and criticality in antiblockaded two-dimensional rydberg atom arrays,” *Phys. Rev. Lett.* **128**, 013603 (2022).
- [39] Philip Kitson, Tobias Haug, Antonino La Magna, Oliver Morsch, and Luigi Amico, “Rydberg atomtronic devices,” *Phys. Rev. A* **110**, 043304 (2024).
- [40] Wan-Xia Li, Jin-Lei Wu, Shi-Lei Su, and Jing Qian, “High-tolerance antiblockade SWAP gates using optimal pulse drivings,” *Phys. Rev. A* **109**, 012608 (2024).
- [41] Hanlae Jo, Yunheung Song, Minhyuk Kim, and Jaewook Ahn, “Rydberg atom entanglements in the weak coupling regime,” *Phys. Rev. Lett.* **124**, 033603 (2020).
- [42] Jin-Lei Wu, Shi-Lei Su, Yan Wang, Jie Song, Yan Xia, and Yong-Yuan Jiang, “Effective rabi dynamics of rydberg atoms and robust high-fidelity quantum gates with a resonant amplitude-modulation field,” *Opt. Lett.* **45**, 1200–1203 (2020).
- [43] Jin-Lei Wu, Yan Wang, Jin-Xuan Han, Shi-Lei Su, Yan Xia, Yongyuan Jiang, and Jie Song, “Resilient quantum gates on periodically driven rydberg atoms,” *Phys. Rev. A* **103**, 012601 (2021).
- [44] Xiao-Qiang Shao, Jin-Hui Wu, and Xue-Xi Yi, “Dissipative stabilization of quantum-feedback-based multipartite entanglement with rydberg atoms,” *Phys. Rev. A* **95**, 022317 (2017).
- [45] André Eckardt, “Colloquium: Atomic quantum gases in periodically driven optical lattices,” *Rev. Mod. Phys.* **89**, 011004 (2017).
- [46] Sagarika Basak, Yashwant Chougale, and Rejish Nath, “Periodically driven array of single rydberg atoms,” *Phys. Rev. Lett.* **120**, 123204 (2018).
- [47] Luheng Zhao, Michael Dao Kang Lee, Mohammad Mujahid Aliyu, and Huanqian Loh, “Floquet-tailored rydberg interactions,” *Nature Communications* **14**, 7128 (2023).
- [48] S. Kumar Mallavarapu, Ankita Niranjan, Weibin Li, Sebastian Wüster, and Rejish Nath, “Population trapping in a pair of periodically driven rydberg atoms,” *Phys. Rev. A* **103**, 023335 (2021).
- [49] Long B. Nguyen, Yosep Kim, Akel Hashim, Noah Goss, Brian Marinelli, Bibek Bhandari, Debmalya Das, Ravi K. Naik, John Mark Kreikebaum, Andrew N. Jordan, David I. Santiago, and Irfan Siddiqi, “Programmable heisenberg interactions between floquet qubits,” *Nature Physics* **20**, 240–246 (2024).
- [50] Lingxiao Zhou, Bin Liu, Yuze Liu, Yang Lu, Qiuyang Li, Xin Xie, Nathaniel Lydick, Ruofan Hao, Chenxi Liu, Kenji Watanabe, Takashi Taniguchi, Yu-Hsun Chou, Stephen R. Forrest, and Hui Deng, “Cavity floquet engineering,” *Nature Communications* **15**, 7782 (2024).
- [51] Kentaro Heya, Moein Malekakhlagh, Seth Merkel, Naoki Kanazawa, and Emily Pritchett, “Floquet analysis of frequency collisions,” *Phys. Rev. Appl.* **21**, 024035 (2024).
- [52] Bao-Jie Liu, Xue-Ke Song, Zheng-Yuan Xue, Xin Wang, and Man-Hong Yung, “Plug-and-play approach to nonadiabatic geometric quantum gates,” *Phys. Rev. Lett.* **123**, 100501 (2019).
- [53] Hang Li, Yang Liu, and GuiLu Long, “Experimental realization of single-shot nonadiabatic holonomic gates in nuclear spins,” *Science China Physics, Mechanics & Astronomy* **60**, 080311 (2017).
- [54] Shuo Ma, Genyue Liu, Pai Peng, Bichen Zhang, Sven Jandura, Jahan Claes, Alex P. Burgers, Guido Pupillo, Shruti Puri, and Jeff D. Thompson, “High-fidelity gates and mid-circuit erasure conversion in an atomic qubit,” *Nature* **622**, 279–284 (2023).
- [55] Xue-Ke Song, Hao Zhang, Qing Ai, Jing Qiu, and Fu-Guo Deng, “Shortcuts to adiabatic holonomic quantum computation in decoherence-free subspace with transitionless quantum driving algorithm,” *New Journal of Physics* **18**, 023001 (2016).
- [56] J. F. Haase, Z.-Y. Wang, J. Casanova, and M. B. Plenio, “Soft quantum control for highly selective interactions among joint quantum systems,” *Phys. Rev. Lett.* **121**, 050402 (2018).
- [57] JinLei Wu, Shuai Tang, Yan Wang, XiaoSai Wang, JinXuan Han, Cheng Lü, Jie Song, ShiLei Su, Yan Xia, and YongYuan Jiang, “Unidirectional acoustic metamaterials based on nonadiabatic holonomic quantum transformations,” *Science China Physics, Mechanics & Astronomy* **65**, 220311 (2021).
- [58] Hong-Da Yin and X. Q. Shao, “Gaussian soft control-based quantum fan-out gate in ground-state manifolds of neutral atoms,” *Optics letters* **46** **10**, 2541–2544 (2021).
- [59] Xue-Ke Song, Qing Ai, Jing Qiu, and Fu-Guo Deng, “Physically feasible three-level transitionless quantum driving with multiple schrödinger dynamics,” *Phys. Rev. A* **93**, 052324 (2016).
- [60] Jin-Lei Wu, Yan Wang, Jin-Xuan Han, Cong Wang, Shi-Lei Su, Yan Xia, Yongyuan Jiang, and Jie Song, “Two-path interference for enantiomer-selective state transfer of chiral molecules,” *Phys. Rev. Appl.* **13**, 044021 (2020).
- [61] Jin-Xuan Han, Jin-Lei Wu, Yan Wang, Yan Xia, Yong-Yuan Jiang, and Jie Song, “Large-scale greenberger-horne-zeilinger states through a topologically protected zero-energy mode in a superconducting qutrit-resonator chain,” *Phys. Rev. A* **103**, 032402 (2021).
- [62] Qiaolin Wu, Jun Xing, and Hongda Yin, “Soft-controlled quantum gate with enhanced robustness and undegraded dynamics in rydberg atoms,” *EPJ Quantum Technology* **11**, 1 (2024).
- [63] Jin-Kang Guo, Jin-Lei Wu, Ji Cao, Shou Zhang, and Shi-Lei Su, “Shortcut engineering for accelerating topologi-



- cal quantum state transfers in optomechanical lattices,” *Phys. Rev. A* **110**, 043510 (2024).
- [64] Lov K. Grover, “Quantum mechanics helps in searching for a needle in a haystack,” *Phys. Rev. Lett.* **79**, 325–328 (1997).
- [65] Lov K. Grover, “Quantum computers can search rapidly by using almost any transformation,” *Phys. Rev. Lett.* **80**, 4329–4332 (1998).
- [66] G. L. Long, “Grover algorithm with zero theoretical failure rate,” *Phys. Rev. A* **64**, 022307 (2001).
- [67] Gui Lu Long, Yan Song Li, Wei Lin Zhang, and Li Niu, “Phase matching in quantum searching,” *Physics Letters A* **262**, 27–34 (1999).
- [68] Gui-Lu Long, Xiao Li, and Yang Sun, “Phase matching condition for quantum search with a generalized initial state,” *Physics Letters A* **294**, 143–152 (2002).
- [69] Xin He, Wen-Tao Zhao, Wang-Chu Lv, Chen-Hui Peng, Zhe Sun, Yong-Nan Sun, Qi-Ping Su, and Chui-Ping Yang, “Experimental demonstration of deterministic quantum search for multiple marked states without adjusting the oracle,” *Opt. Lett.* **48**, 4428–4431 (2023).
- [70] Krishanu Sankar, Artur Scherer, Satoshi Kako, Sam Reifenstein, Navid Ghadermarzy, Willem B. Krayenhoff, Yoshitaka Inui, Edwin Ng, Tatsuhiro Onodera, Pooya Ronagh, and Yoshihisa Yamamoto, “A benchmarking study of quantum algorithms for combinatorial optimization,” *npj Quantum Information* **10**, 64 (2024).
- [71] Zhi-Hao Li, Gui-Fang Yu, Ya-Xin Wang, Ze-Yu Xing, Ling-Wen Kong, and Xiao-Qi Zhou, “Experimental demonstration of deterministic quantum search algorithms on a programmable silicon photonic chip,” *Science China Physics, Mechanics & Astronomy* **66**, 290311 (2023).
- [72] Xiang Li, Hanxiang Shen, Weiguo Gao, and Yingzhou Li, “Resource Efficient Boolean Function Solver on Quantum Computer,” *Quantum* **8**, 1500 (2024).
- [73] Bibek Pokharel and Daniel A. Lidar, “Better-than-classical grover search via quantum error detection and suppression,” *npj Quantum Information* **10**, 23 (2024).
- [74] V. Borish, O. Marković, J. A. Hines, S. V. Rajagopal, and M. Schleier-Smith, “Transverse-field ising dynamics in a rydberg-dressed atomic gas,” *Phys. Rev. Lett.* **124**, 063601 (2020).
- [75] Sebastian Geier, Nithiwadee Thaicharoen, Clément Hainaut, Titus Franz, Andre Salzinger, Annika Tebben, David Grimshandl, Gerhard Zürn, and Matthias Weidemüller, “Floquet hamiltonian engineering of an isolated many-body spin system,” *Science* **374**, 1149–1152 (2021).
- [76] D. X. Li and X. Q. Shao, “Unconventional rydberg pumping and applications in quantum information processing,” *Phys. Rev. A* **98**, 062338 (2018).
- [77] Hannes Bernien, Sylvain Schwartz, Alexander Keesling, Harry Levine, Ahmed Omran, Hannes Pichler, Soonwon Choi, Alexander S. Zibrov, Manuel Endres, Markus Greiner, Vladan Vuletić, and Mikhail D. Lukin, “Probing many-body dynamics on a 51-atom quantum simulator,” *Nature* **551**, 579–584 (2017).
- [78] Harry Levine, Alexander Keesling, Ahmed Omran, Hannes Bernien, Sylvain Schwartz, Alexander S. Zibrov, Manuel Endres, Markus Greiner, Vladan Vuletić, and Mikhail D. Lukin, “High-fidelity control and entanglement of rydberg-atom qubits,” *Phys. Rev. Lett.* **121**, 123603 (2018).
- [79] Michael A Nielsen, “A simple formula for the average gate fidelity of a quantum dynamical operation,” *Physics Letters A* **303**, 249–252 (2002).
- [80] T. Wilk, A. Gaëtan, C. Evellin, J. Wolters, Y. Miroshnychenko, P. Grangier, and A. Browaeys, “Entanglement of two individual neutral atoms using rydberg blockade,” *Phys. Rev. Lett.* **104**, 010502 (2010).
- [81] Bing-Bing Liu, Zheng Shan, M.-R. Yun, D.-Y. Wang, B.-J. Liu, L.-L. Yan, M. Feng, and S.-L. Su, “Robust three-qubit search algorithm in rydberg atoms via geometric control,” *Phys. Rev. A* **106**, 052610 (2022).